# Composite Trough Evolution of Selected West Pacific Extratropical Cyclones

RICHARD GROTJAHN*

*National Center for Atmospheric Research,† Boulder, Colorado*

(Manuscript received 16 May 1995, in final form 17 January 1996)

ABSTRACT

The observed vertical structures of the trough axes for 27 extratropical cyclones are presented. This study is motivated by results from a simple theoretical model. Two observing times during the cyclone life cycle are shown: prior to development and during the "mature" but still amplifying stage. Prior to development, upper and lower troughs are present and separate, each has little or no tilt, the upper one is typically prominent down to 4-km elevation, and the separation between the lower and the upper features varies depending on where the approaching upper trough happens to be at the observing time. At the mature stage, upper and lower features are connected, a uniform tilt typically develops through the entire troposphere, the tilt is typically due west with height, and the tilt may have a preferred slope. An empirical orthogonal function (EOF) analysis finds that two modes account for more than 97% of the variance. The equivalent barotropic EOF has the most variance by far, though the fractional amount diminishes over time as this EOF also extends further downward. The first baroclinic EOF increases fractional amplitude in compensation.

## 1. Introduction

In an earlier paper (Grotjahn and Tribbia 1995; hereafter GT) we presented a general description of how the trough axis may evolve over time for an extratropical cyclone. Figure 1b is a schematic illustration. Grotjahn and Tribbia proposed that the conditions prior to development often consist of an upper-level trough (having little or no upstream tilt with height) and a *separate* lower-level trough (shallow, vertical axis) to the east. As time progresses, the upper trough approaches the lower trough and when the two reach a distance apart that approximates the phase shift of a linear, normal-mode-type structure, then a tilted trough emerges that *connects* the upper and lower features. The normal-mode phase shift also approximates the spacing needed for the divergence pattern ahead of an upper trough to support surface development. The cyclone may maintain this tilt while amplifying and propagating (between times "1" and "2" in the figure). Eventually, the cyclone amplitude becomes so large that nonlinearity dominates. Grotjahn and Tribbia showed an example of this process for a single storm that developed over eastern North America. The example used observations and forecast model output. In this report we intend to verify the generality of some results shown in GT by examining many more cyclones. We also select a different region and focus on cyclones that develop and grow between the east coast of Asia and the dateline.

The purpose in considering the structure of the trough is detailed in GT. Briefly, GT demonstrate, using a simple theoretical model, that the amount of tilt present prior to development strongly affects which of two types of growth mechanism are presumed to apply. If the growth is by a baroclinically unstable normal-mode-type structure, the rapidity with which growth becomes apparent depends upon the amplitude of the normal mode present (i.e., its projection) in the initial conditions. Grotjahn and Tribbia labeled the other type of instability nonmodal growth (NG), as a general term for whatever adiabatic (and nonbarotropic) growth may be occurring during the solution of the initial value problem. An example of NG is schematically illustrated in Fig. 1a. Primarily, this NG could be understood as a structural change that converts one portion of quasigeostrophic potential vorticity (the "thermal" part) into the relative vorticity part. Nonmodal growth includes a shape change, whereas normal mode growth does not. Grotjahn and Tribbia showed that NG was large if a connected and tilted trough becomes tilted into the vertical over time (Fig. 1a); NG was much less if the initial conditions had separate, untilted troughs (Fig. 1b). So, GT examined a single observed storm with the following questions in mind. (a) Were the upper and lower features *un*connected prior to development? (b)

* Permanent affiliation: Dept. of Land, Air, and Water Resources, University of California, Davis, Davis, California.

† The National Center for Atmospheric Research is sponsored by the National Science Foundation.

*Corresponding author address:* Dr. Richard Grotjahn, Dept. of Land, Air, and Water Resources, University of California, Davis, Rm. 151 Hoagland Hall, Davis, CA 95616.
E-mail: quetzal@neit.cgd.ucar.edu

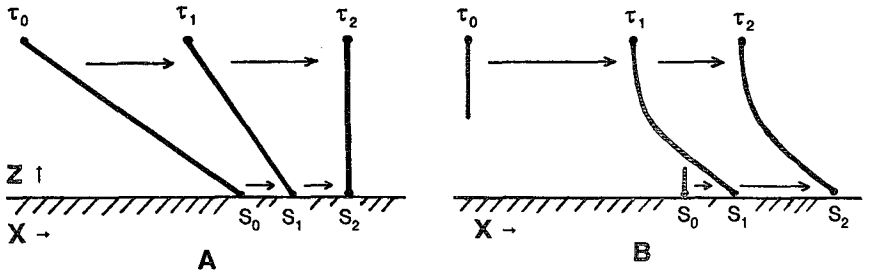


FIG. 1. Longitude versus height schematic cross sections showing an idealized trough axis at three successive times. The endpoints are marked $S$ for surface and $\tau$ for tropopause. Subscripts denote arbitrary units of time: (a) NG example and (b) normal mode example.

Did the trough(s) have little or no tilt prior to development? (c) Did a tilt emerge as the cyclone started to amplify? (d) Did the cyclone maintain a fixed tilt for a time during its amplification? The fourth question requires much higher time resolution than the 12-h observation interval, so GT used a model to consider that question. In GT the answer to each question was "yes." Here, we shall be interested only in studying more cyclones to reconsider the first three questions.

The description presented in the opening paragraph contains many well-known properties. For example, Petterssen and Smebye (1971) describe the most common type of cyclogenesis in similar words (type "B" in their designation). They describe how a preexisting upper-level trough approaches a low-level baroclinic zone. The rising motion ahead of the upper trough (positive differential vorticity advection) reinforces the low-level convergence at the surface trough. Their description contains differences with what we propose. They might call the emergence of a normal mode-type structure a mixed type ("A" and "B") of development. Their type A description keeps the separation between upper and lower trough "sensibly unchanged," whereas in type B it "decreases rapidly." Interestingly, the type B example they show is one they also label as a *mixed* type. What our opening paragraph adds to such standard descriptions is a bit more detail about the trough axis's vertical tilt prior to and during development.

The structure of frontal cyclones has been long studied. So, one would expect that the evolution of so basic a quantity as the trough axis would be well documented in the literature. However, we have been unable to locate a report that explicitly shows the structure for a *collection* of storms. Instead, one easily finds data presented at just two levels and these are usually total fields, from which identifying the perturbation centers is difficult by eye. Examples that show trough information at two levels include: Petterssen and Smebye (1971), Sanders (1986), and Sanders and Gyakum (1980). As is pointed out in GT (and evident here and elsewhere) it would be incorrect to assume that the trough axis varies linearly between sea level and 500 mb (and even worse to extrapolate that trend up to the tropopause). Such details of the trough axis may be outside the scope of previous papers, but it is just those details that are important to a dynamicist, as indicated above.

In other synoptic studies, cross sections of a related variable (like relative vorticity $\zeta$) may be presented. As a rough proxy for the trough axis, one might use the axis of maximum $\zeta$. Bosart and Lin (1984; their Fig. 11) present cross sections of semigeostrophic potential vorticity at times before and during the explosive growth of the "Presidents' Day" storm. In conjunction with contour plots of geopotential height at three levels (their Fig. 1), a case is easily made that the upper and lower features are unconnected and essentially vertical. At the latest of the three times shown the storm has become strong, the upper and lower troughs are connected, and an upstream tilt has developed.

## 2. Analysis techniques

Analysis of the trough axes consists of several steps. A set of criteria is used to choose or exclude a given cyclone. Next, an interpolation domain is chosen to carefully avoid nearby troughs while containing all of the chosen features at four levels. A "background" field is calculated by interpolation across the domain; the difference between that and the total field defines the perturbation. The success of the interpolation is visually checked at three other levels. Finally, trough centers of the perturbation field are objectively found at all levels on a high-resolution grid.

The data used in this study are geopotential height provided by The National Meteorological Center (NMC, now known as the National Centers for Environmental Prediction) and archived at the National Center for Atmospheric Research (NCAR) using T42 resolution. The NCAR CCM post processor (Buja 1994) was used to interpolate this data onto 10 pressure levels and T106 horizontal resolution. The pressure levels are not equally spaced. The pressure levels are spaced approximately 1 km apart, starting at 1 km elevation and extending to 10 km. The matching of

heights to pressure levels is based on the winter, midlatitude U.S. standard atmosphere (USCESA 1976) profiles. For reference, the 1-km level is 899 mb, while the 10-km elevation is 265 mb. Four recent winter periods were examined, from which 27 cases were isolated.

The criteria used to select cases are as follows. A storm must be "primary" development, not a "secondary" storm developing close to a parent cutoff low. The close proximity of a parent low can make the perturbation hard to isolate by any choice of interpolation domain. Troughs that are already strong as they move out of central Asia are excluded since we are interested in identifying conditions prior to as well as during cyclogenesis. Cyclones that develop too far west are excluded if the interpolation domain would need to extend west of 95°E. This criteria avoids cases where too much of the domain at low levels is intercepted by topography. Cyclones that develop too far east are excluded if the interpolation domain would extend east of 180° longitude. Cyclones that follow a track having a large poleward component were excluded because such a track would not work well with some interpolation schemes that we tested, but ultimately did not use. Situations where multiple lows are present with comparable strength were also excluded because of the ambiguity created for the trough selection scheme. (The scheme may toggle between the two low centers at successive levels, and successive times.) However, as noted below, instances where a second upper trough merges with the original trough, and one becomes much stronger than the other, are kept. The cyclone must start from a very weak surface low, commence development, and continue to be growing during five observing periods (48 h). Cyclones that develop some type of upstream tilt are selected. Specifically, during the time period two examples of equivalent barotropic cyclones (which amplify) were noted and excluded by this criterion. To provide some uniformity in comparing different troughs having different tracks, we excluded cyclones that tracked too far north or south, favoring the majority that track over or just south of Japan. During the winters studied, roughly half of the cyclones met *all* these criteria.

The scheme used for defining the perturbation (i.e., for isolating the traveling trough) is key. Analyzing the total field by eye is too subjective and it is almost impossible to see the trough *center* since the upper feature consists of a roughly circular feature embedded onto a meridional trend in geopotential height. The problem is exacerbated when trying to find the weak short-wave trough prior to development. Relative vorticity could be used, but it is an imperfect proxy. For one thing, the strong subtropical jet introduces a meridional trend in $\zeta$. For another, the axis of maximum $\zeta$ does not necessarily line up with the trough axis.

Several schemes were tried to calculate the perturbation height. First, removing the zonal mean does not work because the large height gradients remain from the strong Asian subtropical jet. Second, removal of the longest wavenumber (and scale index) spherical harmonics components was the worst definition, resulting in perturbation fields with minima that bore little relation to subjective expectations. Third, removal of the local time mean was inadequate. The data used in the time mean were centered about each observing time. Several averaging periods were tried ranging from 5 to 29 days. This approach failed because (a) changes over time seen in the perturbation were partly due to variations in the mean being removed and (b) the time mean being removed also included the large amplitude mature stage of the same storm. Fourth, we tried removing zonal means over limited sectors. The sectors could not be geographically fixed without obtaining a strong influence from the Aleutian low. Sliding sectors that were centered around the perturbation did not work because the lack of meridional interpolation created strong, artificial boundaries along the north and south edges of the sectors.

The best procedure was to perform a bilinear interpolation (with greater weighting to the longitude direction) across a manually defined domain that included all of the trough at all levels. The domain was placed so that the interpolation left a background pattern that flowed smoothly across the domain. Figure 2 shows a typical example of the perturbation, background, and total fields obtained by this scheme. At 200 mb, for example, this procedure usually defined the domain to extend from the "inflection point" in the height contours ahead of the trough to the similar point behind the trough. A domain must be specified for each time and each trough. So, the 27 cases studied at five observing times required 135 separate domain definitions. An additional difficulty is to make sure each specified domain works adequately at all levels. When specifying each meridional boundary, one must compromise between two preferences: that total field contours be as straight as possible there and that the domain encompass an area of fairly uniform geopotential height gradient.

The interpolation scheme we used required the most amount of manual intervention of all the schemes tested. While the manual specification was tedious, this scheme does have some benefits. The perturbation trough location was found to be not sensitive to small changes in the choice of domain boundaries. The manual intervention required examination of the calculated fields so that unreasonable perturbation and background flows could be identified and rejected. Finally, perturbation and background patterns with the desired properties could be obtained without any smoothing or any other alteration of the data.

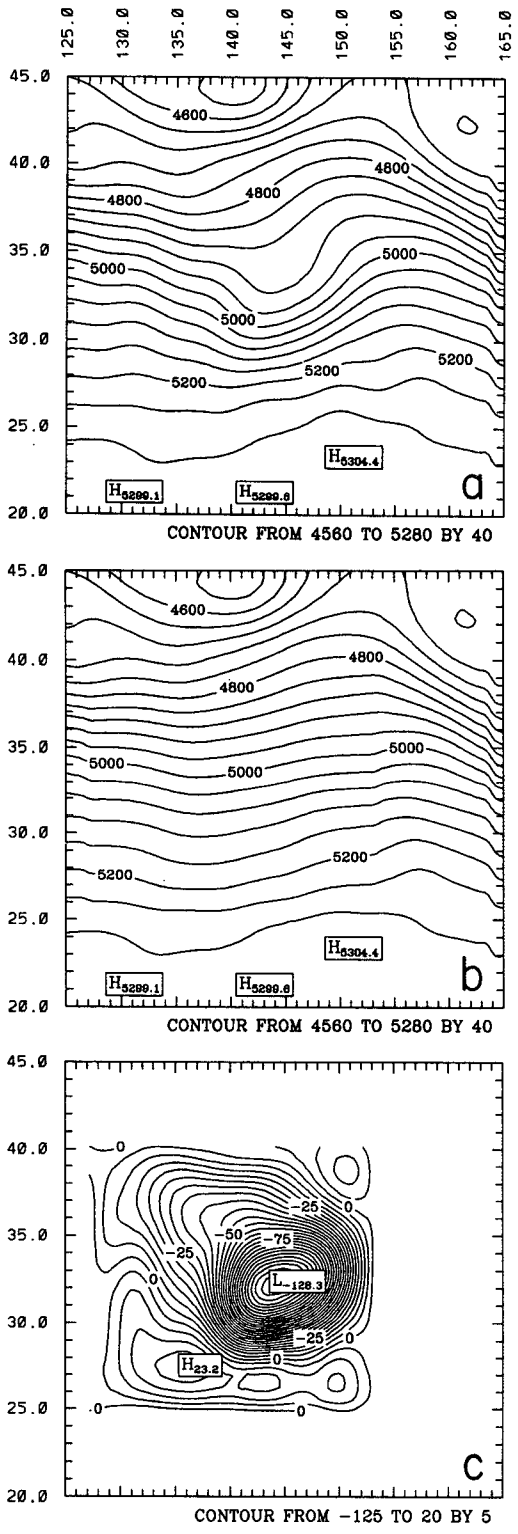


FIG. 2. Geopotential height fields at 540 mb for 0000 UTC 12 January 1994: (a) total field, (b) background field obtained from bilinear interpolation that weights zonal more heavily than meridional direction, and (c) the difference between (a) and (b). The bottom diagram is the perturbation field. Units are meters.

## 3. Composite results

### *a. Predevelopment and mature trough axes*

The trough axes for the perturbation geopotential height are diagramed in the next two figures. The axes for the situation prior to the onset of development are discussed first. We call this stage the "predevelopment" stage. The predevelopment data time chosen depends upon how well the trough is identifiable in the perturbation fields (similar to Fig. 2c, except at four levels). The other criterion is that the surface low have little or no deepening over the prior data interval. The discussion then moves to the axes of the storms that are at a "mature" stage. Depending upon how rapidly the development proceeds relative to the observing times, the mature stage selected is 12–48 h (most are 24 h) after the corresponding predevelopment time. Note that each storm amplifies during both the 12 h before and after the mature stage (as measured by deepening of each storm's sea level central pressure).

The trough axes for the predevelopment state are presented in Fig. 3. The view is from the north, looking south; east is left, west is right. Figure 3a shows the actual trough locations shifted horizontally so that they begin at the same point at the 899-mb (1 km) level. The plotted domain extends for 45° longitude and nearly 35° latitude. The vertical coordinate is essentially geometric height, and extends from 0 to 10 km. The trough axis locations were calculated at the 10 integer multiples of 1 km. However, to expand the vertical scale of the plot, the value at each intermediate level was set equal to the value at the next calculated level above. (The value at 1.5 km is set to the value at 2 km, the value at 2.5 equals that at 3 km, etc.) Furthermore, the trough locations are found to the nearest grid point, which at T106 resolution is slightly more than 1° in each direction. Both procedures produce the "jaggedness" seen in the lines. To better see the 3D trough shape, projections of each axis are plotted on the bottom (dashed lines in Figs. 3a–e and 4a–e) and on the meridional plane.

Many of the axes in Figs. 3a–e have at least three simple properties in common. First, most troughs have an upper portion that is nearly vertical. This result is consistent with the single case studied by GT. The upper troughs extend down to at least 4-km elevation. Second, the vast majority of the troughs have an upper portion that is located not only west, but also *north* of the lower-troposphere location. A portion of this orientation is due to the long-wave trough centered to the east. Many of the upper-level troughs follow the northwesterly flow existing prior to development. However, it is common for the low-level trough to migrate northward at the same time that the upper feature has a southward propagation component. Third, the upper portion of the trough is distributed somewhat evenly along an orientation roughly northwest from the lower-troposphere location. This property is consistent with a sep-

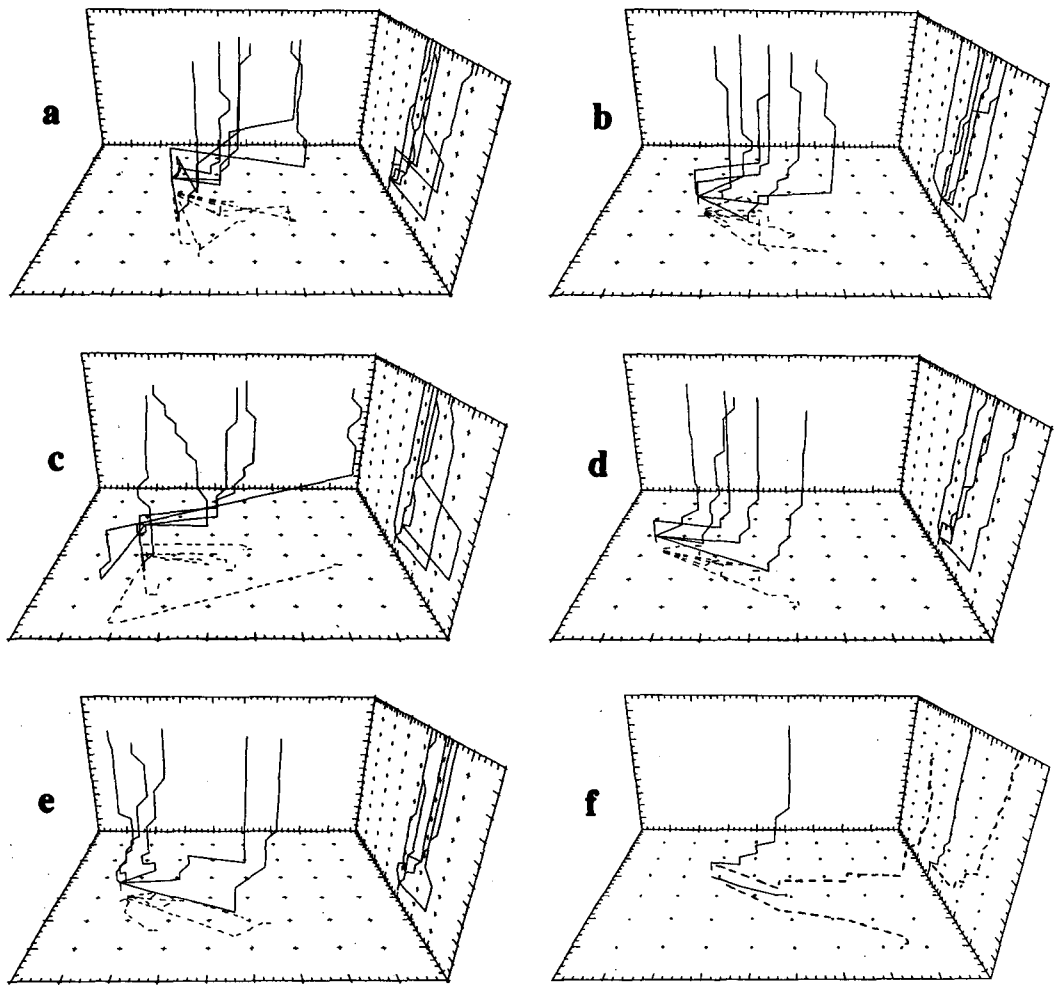


FIG. 3. Perspective view of trough axes prior to development looking from the north toward the south. (a)–(e) Twenty-seven individual troughs plotted so that all troughs have their center at 899 mb drawn at the same place. The region is 45° longitude by 35° latitude. The vertical coordinate is height, with the top located at 10 km. The solid lines within each box are the 3D axes. To see the 3D structure better, 2D projections are drawn on the bottom (dashed lines) and meridional plane (solid lines on right side of each box). Dots are drawn at intervals of 5° latitude and longitude. (f) Similar to the other five plots except that two 3D axes are plotted. The solid line is the average position of the trough at each level using the data in the other five plots. The dashed line (within the box) applies a stretching multiplier to each axis shown in diagrams (a)–(e) prior to taking the average. Projections are also drawn for these two curves.

arate upper feature that is sampled at apparently random times as it approaches the lower-level frontal cyclone.

In Fig. 3f are plotted two curves. The solid line is simply the average at each level of the trough locations shown in Fig. 3f. This line has several purposes. One use is to calculate standard deviations from this mean at each level. The dashed line shows the average at each level when a stretching factor multiplies the longitudinal distance separating the surface position and the position at a given level. The multiplier varies with the case so that the longitudinal distance between the *endpoints* of each trough becomes the same in each case. The same multiplier is used to stretch the meridional direction, too. If the upper-level feature is essentially vertical, then the stretching should not change that. The dashed line does indeed show a vertical trough axis through most of the troposphere. At and above 4-km elevation, the average trough axis in both averaging schemes appears to be vertical, and just displaced in the horizontal.

Figure 4 shows mature cyclone trough axes using the same depictions as in the previous figure. The size of the domain is the same as before. Several simple properties are evident. The majority of the axes tilt to the west with height, and most have comparatively small meridional tilt. To some extent, meridional tilt must be reduced by a selection procedure that avoids cyclones

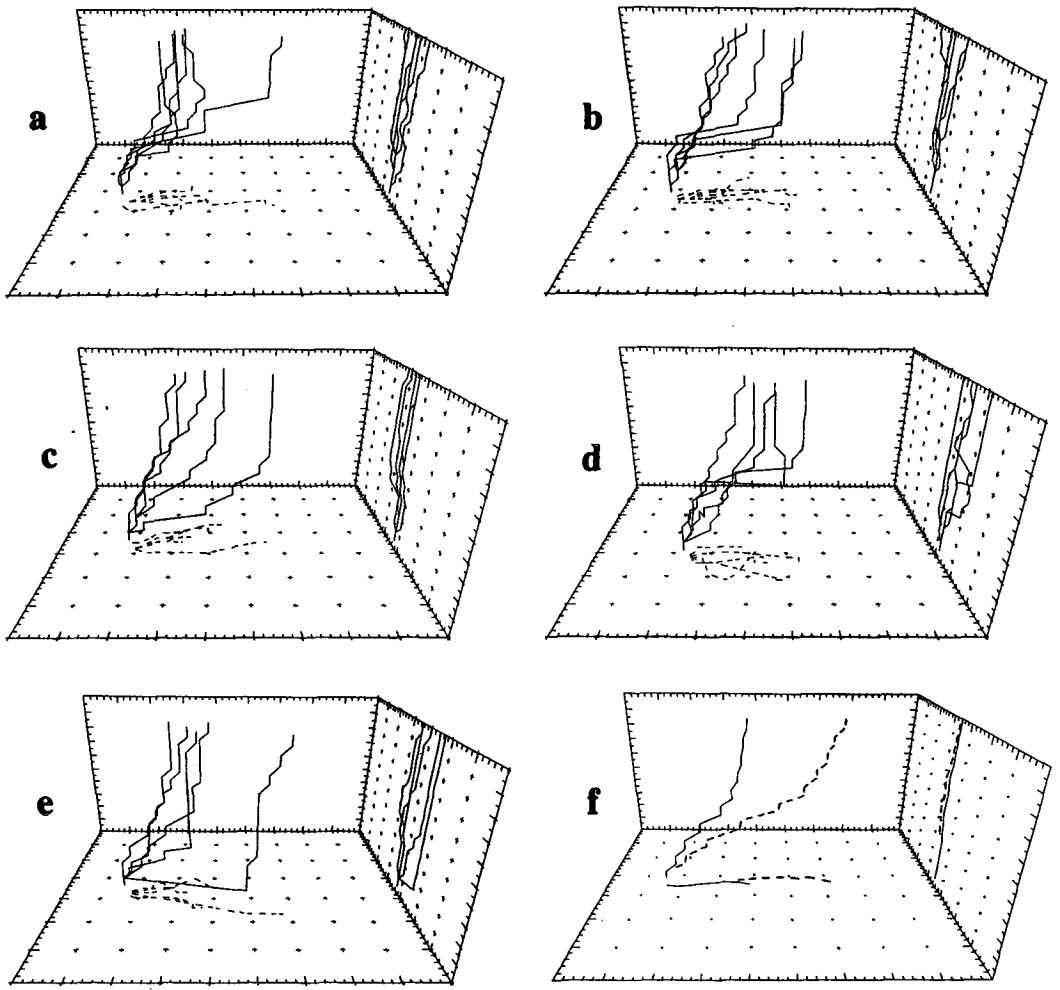


FIG. 4. Same as Fig. 3 except for troughs at the mature stage of development.

that have a strong northward track. However, the selection procedure is unlikely to be a dominant effect because there is much greater meridional scatter at the earlier time (Fig. 3a–e). The majority of the troughs have a similar amount of tilt with height. The trough locations in the upper troposphere are not as widely scattered as in the previous figure. Note that the mean longitudinal displacement in Figs. 3f and 4f (solid lines) is roughly the same. Hence, the standard deviation of the trough locations at the top level in Figs. 3a–e and 4a–e is much less during the mature stage. The dashed line shows the stretched trough average calculated using the same procedure as before. It is noteworthy that the stretching does affect the mature trough. Whereas Fig. 3f indicated that the upper trough was essentially vertical in the majority of cases, here it indicates a tilted trough in the majority of cases. Hence, between the data times used in Figs. 3 and 4, each initially untilted trough has developed tilt.

In Figs. 3 and 4, only the deepest trough at each level is identified. This scheme shows the tilt well, but it does not present convincing evidence for unconnected trough axes except when the trough axis has so large a change between successive levels that a single trough seems unlikely. Many of the troughs in Figs. 3a–e contain such a large change but perhaps not all. The separateness of the upper and lower troughs prior to development is more apparent in horizontal plots of geopotential height. Figure 5a illustrates the point using three levels. The upper and lower levels only have one trough. The intermediate level shown has two troughs, each is nearly colocated with either the upper or the lower trough. To complete the argument, Fig. 5b shows the same cyclone during its mature stage. The mature cyclone has a single trough at all levels and its position varies smoothly with height between all levels tracked (including levels not shown).

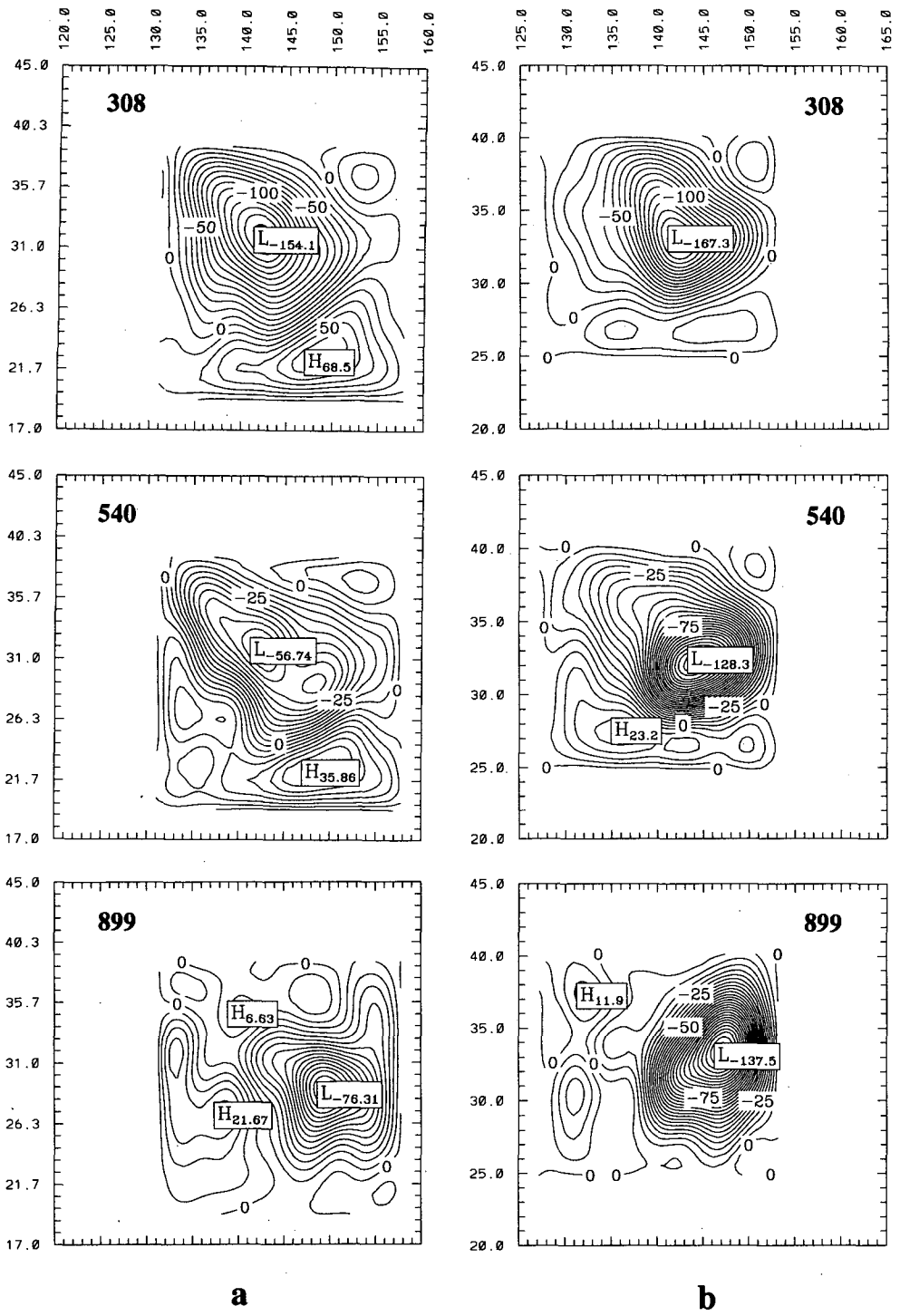


FIG. 5. Perturbation geopotential height $Z'$ at three levels: 308 hPa (top), 540 hPa (middle), 899 hPa (bottom). (a) Values at 1200 UTC 11 January 1994 and (b) values 12 h later.

The mature stage figure is consistent with the emergence of a normal-mode-type instability that has a preferred amount of upstream tilt with height. If the tilt were continuously decreasing, as predicted by NG, then one would expect a similar amount of longitudinal scatter in the predevelopment and mature stages. This is

not strongly visible. We were cautious to state above (and in more detail in GT) that the period of time during which linear, normal mode dynamics might be applicable is likely to be limited during the development of a given storm. Our premise is that it requires time for a normal-mode structure to emerge from a preceding condition of separate, untilted troughs; and that as the cyclone amplifies, diabatic and nonlinear processes become more and more important. This period of time (call it the "linear" time period) is comparable to the 12-h sampling interval. Therefore, some of the variation seen in Figs. 4a–e *could* result from how close the observing time is to the presumed linear time period.

Another source of scatter for the mature trough locations is created by interaction with other short-wave troughs upstream. As the analysis procedure indicated, we do retain instances where a second trough enters from upstream and becomes the dominant trough at a later time. In Fig. 6 we present two series of schematic diagrams to illustrate how the troughs typically evolve. The view is from the southeast, looking northwest. A three-dimensional perspective is used. Two scenarios are displayed. In the upper group of diagrams an equivalent barotropic upper trough enters from the northwest (Fig. 6a). A shallow surface feature is also present. In Fig. 6c a connected trough has formed that has even tilt with height, as implied by many of the curves in Figs. 4a–e. The intermediate time (Fig. 6b) consists of intermediate properties that are consistent with an emerging normal mode as seen in theoretical models (e.g., Grotjahn et al. 1993). If one inspects the perturbation height fields at the first two stages, one usually finds two separate minima at an intermediate level (recall Fig. 5a) to which the upper and lower features both extend. By the stage shown in Fig. 6c, there is one distinct minimum at each level.

The schematic diagrams shown in Figs. 6d–f illustrate the situation when a trailing trough interacts. The first stage is the same as before. At the middle stage (Fig. 6e) a second trough is visible upstream (to the left). The upstream trough then reinforces the western side of the first upper trough leading to the apparent reemergence of what appear to be separate, nearly vertical upper and lower troughs (Fig. 6f and some troughs in Figs. 4a–e). At subsequent times, if a third trough does not enter, a single tilted trough typically reestablishes and evolves to a state similar to Fig. 6c.

We attempt to quantify the amount of scatter by calculating the standard deviation about the mean (solid lines) shown in Figs. 3f and 4f at each level. We treat the longitudinal and meridional components separately. Recall that the predevelopment and mature sets have nearly the same mean longitudinal distance from the fixed location at 899 mb. The standard deviation at 265 mb in the longitudinal direction is about 9° for the predevelopment set and about 4.5° for the mature set. If we remove the six furthest outliers of both sets, the difference in standard deviations is even more pronounced.

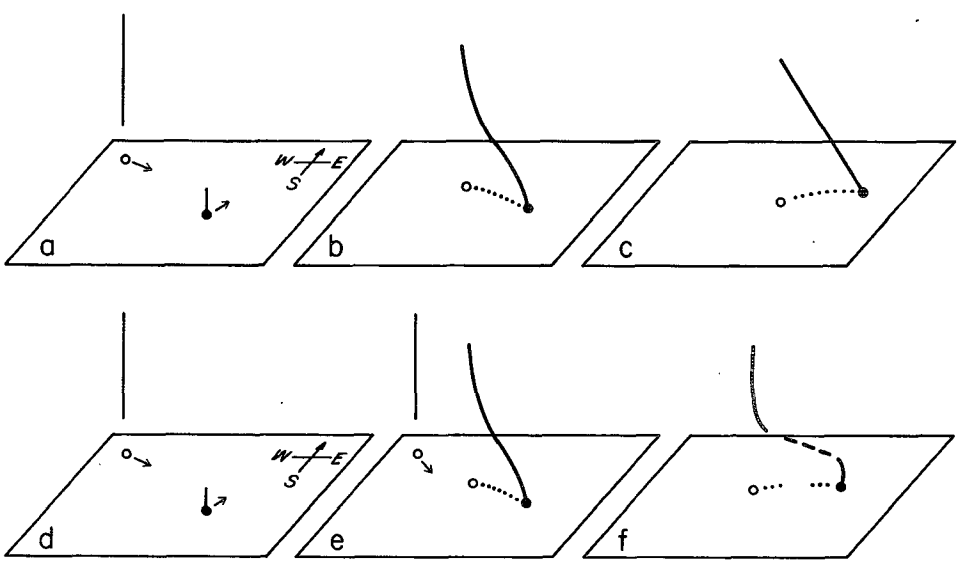


FIG. 6. Schematic evolution of troughs (solid lines) using a perspective view, this time looking from the southeast toward the northwest. The open circles mark where the top of the trough would be when projected onto the earth's surface. The darkened circle is the trough center at the surface. Dotted lines show the projection of intermediate levels of the trough onto the surface. Earliest times are on the left, latest times on the right. Two types of evolution are depicted. Both depictions start with a deep upper trough to the northwest and a shallow, low-level trough to the southeast. In the lower diagram a second upper trough enters from the northwest and merges with the first.

*b. EOF analysis*

One concern about plotting a trough axis using only the minimum perturbation geopotential height at each level is that the horizontal structure may vary considerably from level to level. For example, the axes of a trough and its preceding ridge do not necessarily have the same tilt. Another example would be if the horizontal tilt varied strongly between levels. However, visual inspection of the time mean perturbation fields (shifted as in Figs. 3 and 4 so that trough centers at 899 mb are colocated) reveals perturbation height patterns that are remarkably circular and similar at each level. Hence, the trough axis using the center point will be representative of the vertical structure of the broader region encompassing the whole trough.

The concern about representativeness of the trough axis may be addressed by performing an empirical orthogonal function (EOF) analysis. EOF analysis of atmospheric data is a powerful tool in common use since Kutzbach (1967). The EOFs are calculated from the covariance matrix between perturbation values at every level and summed over all grid points in the horizontal interpolation domain. An introduction to the method may be found in appendix B of Peixoto and Oort (1992).

The EOFs for the 27 case average perturbation fields are presented in Fig. 7. Since we have 10 levels, there are 10 EOFs. In terms of the amount of variance represented, the first two EOFs contain the vast majority. The largest EOF is barotropic and usually has larger amplitude in the upper atmosphere in response to the larger amplitude in geopotential height at upper levels. Figure 7a gives an impression of how the barotropic EOF varies during the onset of development. In proceeding from predevelopment (solid line) to mature (dotted line) stages, the barotropic EOF tends to develop proportionally more amplitude in the lower levels. This EOF accounts for 98.1% (predevelopment) then 93.5% (mature) of the total variance.

The first baroclinic EOF (having one zero crossing) is the next largest. Presented in Fig. 7b, this EOF accounts for 1.7% (predevelopment) then 6.3% (mature) of the total. Typically, this EOF is largest at the bottom level, and is thus more keyed to the location of the low-level trough. While the baroclinic EOF has much less of the variance, the squared nature of this quantity may exaggerate the difference.

As an alternative, one may consider the perturbation geopotential height field $Z'$. Working with $Z'$ (not shown) avoids the squared magnitude comparison. Some sense of the distribution of $Z'$ amplitude may be deduced from the minimum values at three representative levels. Prior to development, $Z'$ has peak negative values of −47 m (at 1 km), −143 m (at 5 km), and −226 m (at 9 km). At the mature stage, $Z'$ has peak negative values −187 m (at 1 km), −181 m (at 5 km), and −250 m (at 9 km).

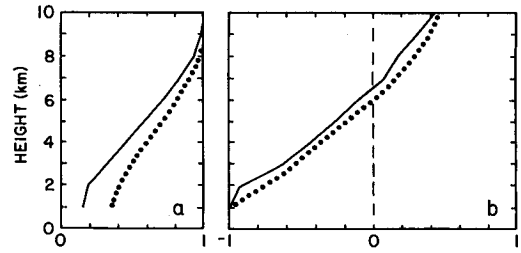


FIG. 7. Normalized vertical structures of the first two EOFs derived from the 3D perturbation geopotential height ($Z'$) field computed by averaging the 27 cases. These two EOFs account for more than 97% of the total variance. Two times are shown: predevelopment (solid lines) and mature stage (dotted lines). (a) The barotropic EOF and (b) the first baroclinic EOF.

Each EOF may be projected onto $Z'$ and then a portion of the height field due to that EOF may be plotted and examined. For the first two EOFs, those projection fields are simple enough to describe in words. The barotropic EOF carries most of the variance and looks much like the $Z'$ field in the upper troposphere. Its peak projection is −233 m (predevelopment) then −247 m (mature). The first baroclinic EOF has peak values of −34 m (predevelopment) then −126 m (mature). The emergence of the tilt is reflected in the large gain by the second EOF relative to the first. The projection pattern of the second EOF has largest negative values roughly where the lower trough is located and positive values to the west, roughly where the surface high is forming. Judging by the baroclinic EOF structure, this mode is picking up higher $Z'$ values both at the surface (to the west of the low) and near tropopause level (generally above the lower trough). The total fields (not shown) have the ridge at 9- and 10-km elevation located east of the trough at 1 km. The third EOF (not shown) has peak values at top, bottom, and near the middle levels; its projection has peak values of 14 m (predevelopment) and 15 m (mature).

The discussion above considered the aggregate of the 27 cases. Considering a single case is also informative. As our example, we chose a time period (11–12 January 1994) with trough evolution that is quite similar to the schematic development indicated in Figs. 6a–c. The first two EOFs again dominate, but they are a bit more evenly matched. Here we focus on the time evolution for three successive times (starting with a predevelopment state and ending with a mature state). The variance accounted for by the barotropic EOF is 86.1, 82.9, then 81.5% as time progresses. In terms of peak amplitude of the projection for this EOF, the $Z'$ values are −71, −91, and −95 m. Between the first and second times discussed, the amplitude profile of this EOF changes similar to Fig. 7a; however, by the latest time, this EOF has roughly uniform amplitude with height. Turning to the second EOF, the variance accounted for by the baroclinic EOF is 11.5%, 15.8%, then 17.3% as

time progresses. In terms of peak amplitude of the projection for this EOF, the projected $Z'$ values are $-36$, $-36$, and $-54$ m. The amplitude profile of this EOF looks similar to Fig. 7b, except that as time proceeds, the relative amplitude at the top grows to become comparable with the amplitude at 1 km. These numbers do not reveal that there is cancellation between the projected fields from respective EOFs. These numbers also do not reflect diminished cancellation over time in favor of more reinforcement. Consequently, the total $Z'$ values at (1, 5, and 9 km) start at ($-39$, $-30$, and $-70$ m) in the predevelopment stage. At the intermediate time the total $Z'$ becomes ($-57$, $-34$, and $-90$ m). At the mature stage total $Z'$ becomes ($-91$, $-82$, and $-98$ m). Amplitude growth at the middle levels lags until the two troughs (one from the upper and one from the lower feature) merge into a single minimum.

## 4. Summary

Trough axes have been analyzed for 27 cases of extratropical cyclogenesis. The cases were selected using criteria that isolate cyclones prior to as well as during development. A bilinear interpolation scheme is used to isolate a perturbation geopotential height field from the larger scale pattern. Once found, it is a simple matter to identify the trough center and several of its properties.

The study was motivated by work in theoretical dynamics. Theory suggests that the amount of tilt present prior to as well as during development is a significant indicator of what processes may be most responsible for the early growth of the cyclone. A previous study (Grotjahn and Tribbia 1995) found the predevelopment state to consist of separate upper and lower troughs, each having little or no tilt, for a single case of cyclogenesis over North America. As the storm began to develop, an upstream (westward) tilt with height emerged and persisted for 12–24 h. One goal of this study is to see if the situation found in GT is unusual or common. Since we are motivated by a specific theoretical dynamics issue we have focused on trough axis evolution and not repeated classical interpretations of development that examine divergence or isentropic potential vorticity fields.

Nearly all of the 27 cases we study share similar properties with the storm described in GT. Prior to development there is much scatter in the location of the upper trough relative to the lower trough (though generally upstream). The scatter is explained as the result of where the approaching upper trough (not connected to the surface feature) happens to be when the observing time occurs for different cyclones. In addition, we find some evidence of a preference for a specific amount of tilt during the mature stage. The lack of scatter at the mature stage does not prove, but is consistent with the theoretical notion of an emerging normal mode. An EOF analysis shows how the trough at lower and middle levels amplifies as the tilt emerges. The perturbation geopotential height ($Z'$) field is largely depicted by the first two EOFs. The first baroclinic EOF leads to the formation of a trailing surface high and a leading upper ridge relative to the trough. The upper ridge is not centered above the lower trough, but leads it, because a large equivalent barotropic EOF is also present. The equivalent barotropic EOF is the largest. As the cyclone evolves the baroclinic EOF gains variance at the expense of the barotropic, reflecting how the initially vertical (equivalent barotropic) upper trough, which has larger amplitude relative to the initial low-level trough, merges with the lower trough and the single trough formed develops upstream (primarily westward) tilt with height.

*Acknowledgments.* The author performed this research while on sabbatical at NCAR. He is grateful for the financial and computing resources provided by the Climate and Global Dynamics division, which sponsored his stay. He is thankful for a wide variety of assistance from the NCAR staff. Particular thanks are directed to J. Tribbia, G. Branstator, L. Buja, and J. Lee. The author appreciates the helpful comments by the anonymous reviewers.

## REFERENCES

Bosart, L., and S. Lin, 1984: A diagnostic analysis of the Presidents' Day storm of February 1979. *Mon. Wea. Rev.*, **112,** 2148–2177.

Buja, L., 1994: CCM modular processor user's guide. NCAR Tech. Note NCAR-TN-384+IA, 239 pp.

Grotjahn, R., and J. Tribbia, 1995: On the mechanism of cyclogenesis as deduced from vertical axis tilts. *Tellus,* **47A,** 629–637.

——, R. Pedersen, and J. Tribbia, 1993: On continuum and normal modes in cyclogenesis. Preprints, *Ninth Conf. on Atmospheric and Oceanic Waves and Stability,* San Antonio, TX, Amer. Meteor. Soc., 31–32.

Kutzbach, J. E., 1967: Empirical eigenvectors of sea level pressure, surface temperature and precipitation complexes over North America. *J. Appl. Meteor.,* **6,** 791–802.

Peixoto, J., and A. H. Oort, 1992: *Physics of Climate.* American Institute of Physics, 492–496.

Petterssen, S., and Smebye, 1971: On the development of extratropical cyclones. *Quart. J. Roy. Meteor. Soc.,* **97,** 457–482.

Sanders, F., 1986: Explosive cyclogenesis in the west-central North Atlantic Ocean, 1981–1984. Part I: Composite structure and mean behavior. *Mon. Wea. Rev.,* **114,** 1781–1794.

——, and J. Gyakum, 1980: Synoptic–dynamic climatology of the "bomb." *Mon. Wea. Rev.,* **108,** 1589–1606.

U.S. Committee on Extension to the Standard Atmosphere (USCESA), 1976: *U.S. Standard Atmosphere 1976.* U.S. Govt. Printing Office, 227 pp.